THE OHIO STATE UNIVERSITY

FE0026334: ADVANCED CONTROL ARCHITECTURE AND SENSOR INFORMATION DEVELOPMENT

FOR PROCESS AUTOMATION, OPTIMIZATION, AND IMAGING OF CHEMICAL LOOPING SYSTEMS

Tien-Lin Hsieh

Andrew Tong (PI), Umit Ozgunner (Co-PI), Arda Kurt (Co-PI)

Department of Chemical and Biomolecular Engineering

2017 Combined Project Portfolio Review| 20 March 2017

Chemical Looping: Fossil Fuel Conversion with Carbon Capture

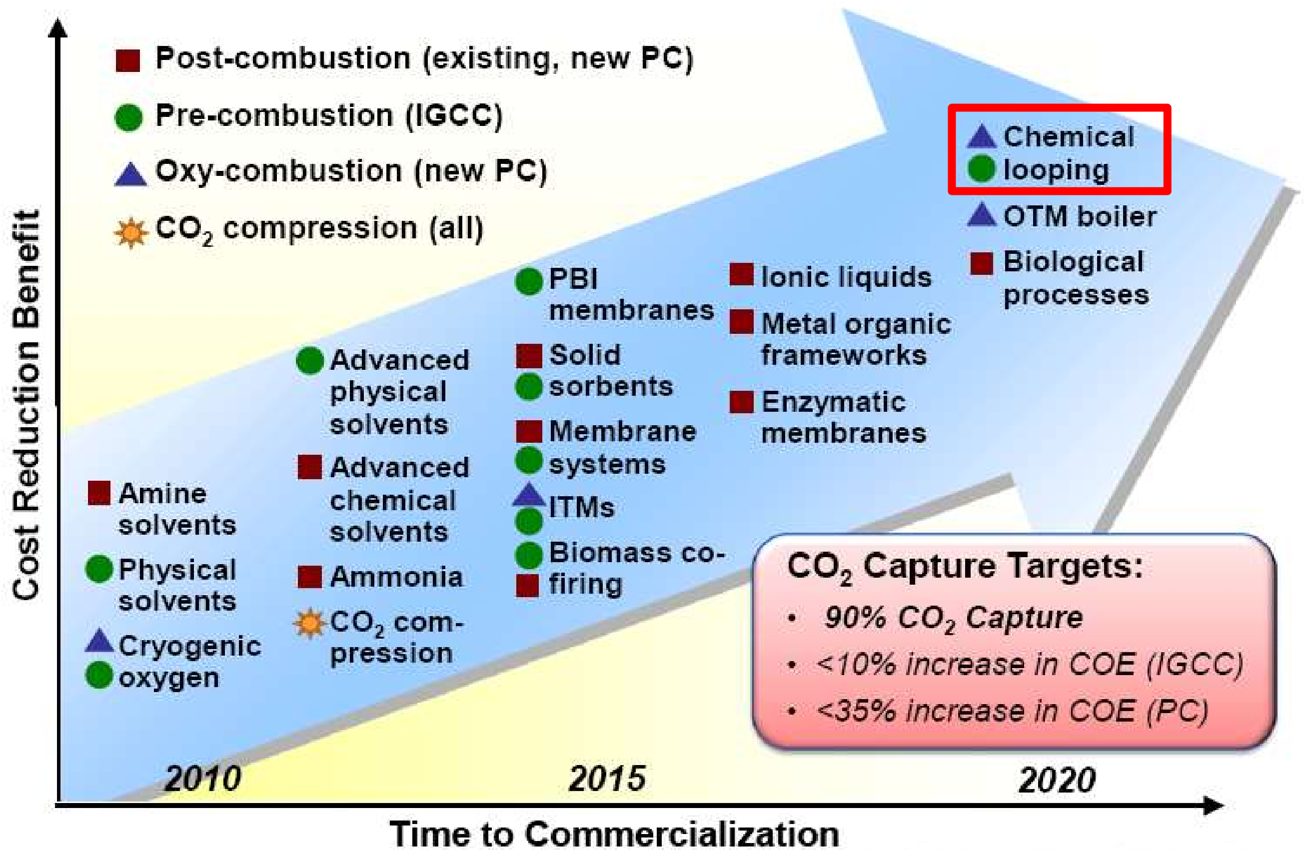

José D. Figueroa, National Energy Technology Laboratory (NETL), U.S. DOE

Applying chemical looping to coal-based hydrogen production

Conventional coal-based hydrogen production w/ carbon capture

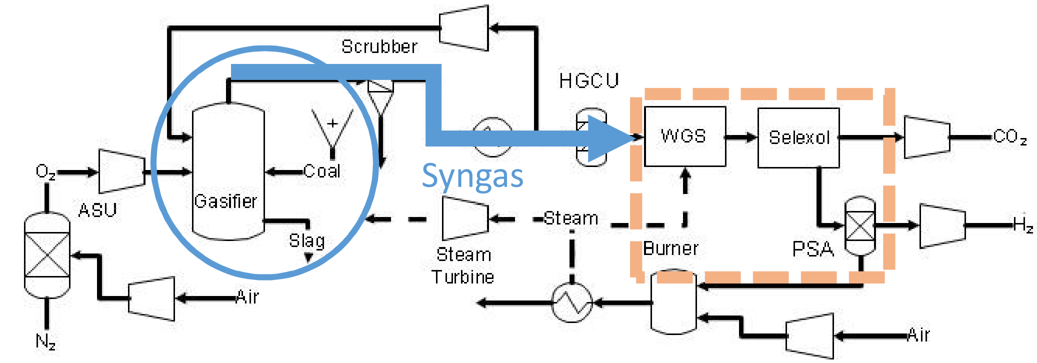

Chemical looping hydrogen production w/ carbon capture

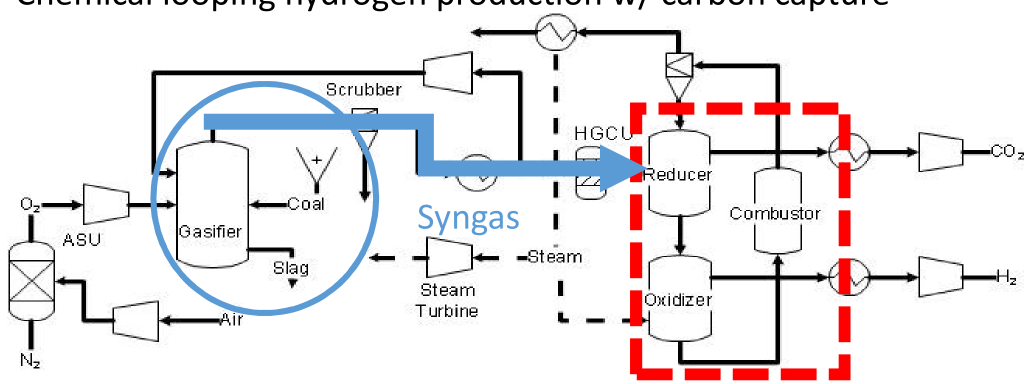

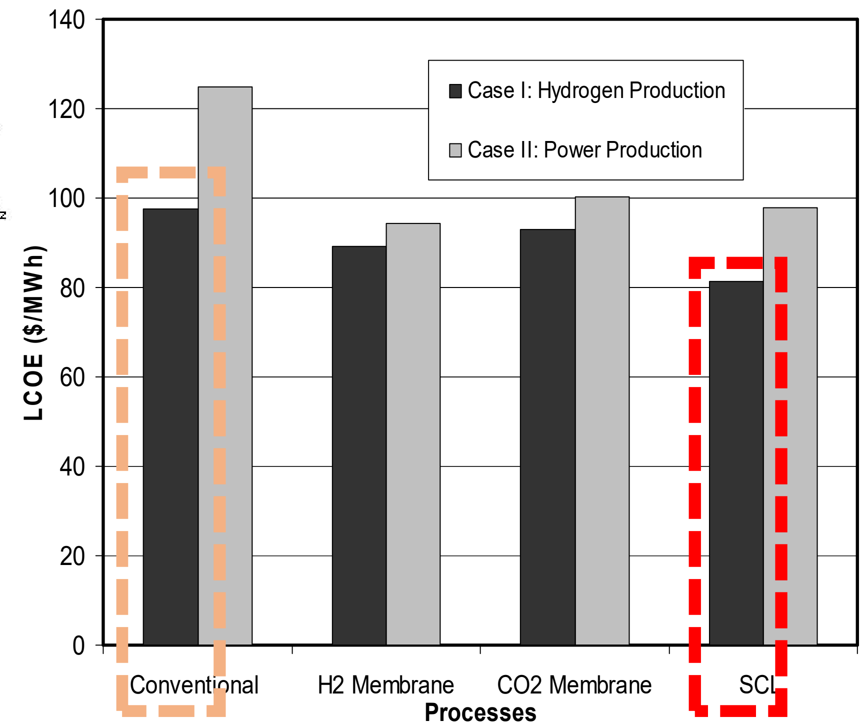

Li, F., Zeng, L., & Fan, L. S. (2010). *Industrial & Engineering Chemistry Research*, *49*(21), 11018-11028.

Syngas Chemical Looping (SCL) Process for H_2 Production

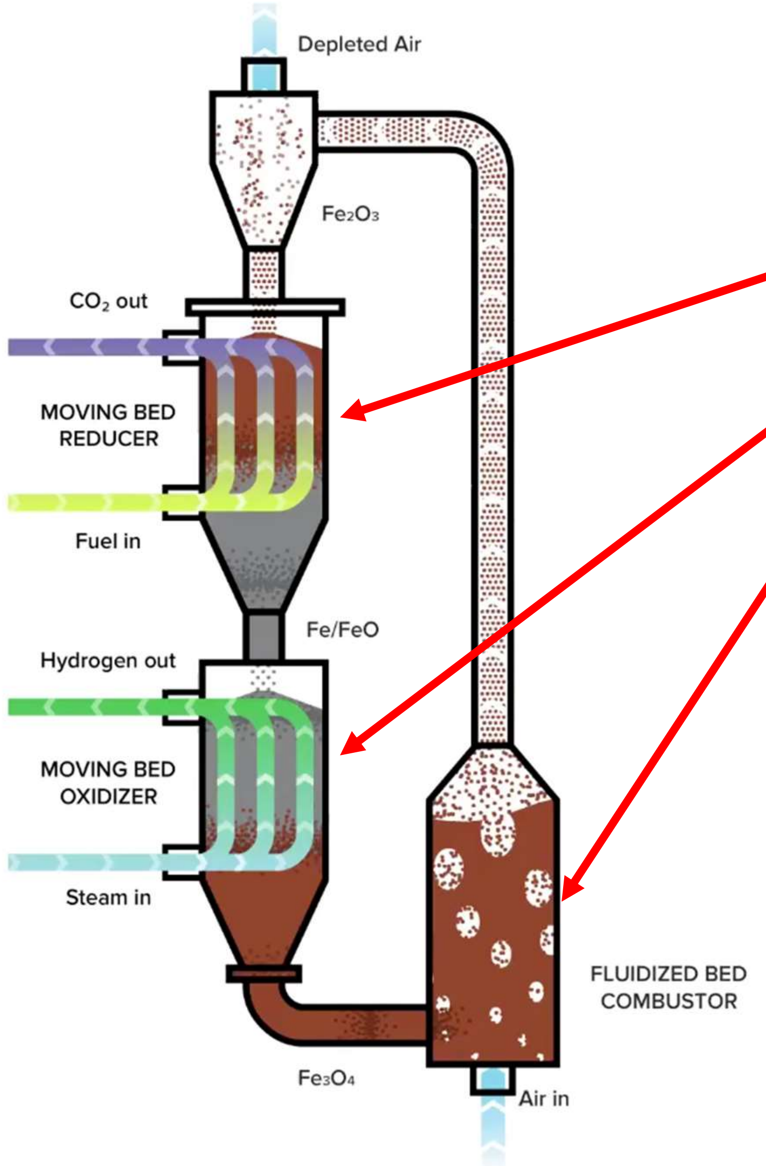

Main reactions:

Reducer:	$C_xH_yO_z + Fe_2O_3 \rightarrow CO_2 + H_2O + Fe$
Oxidizer:	$Fe + H_2O \rightarrow Fe_3O_4 + H_2 + Q$
Combustor:	$Fe_3O_4 + O_2 \rightarrow Fe_2O_3 + Q$
Total:	$C_xH_yO_z + H_2O + O_2 \rightarrow CO_2 + H_2 + Q$

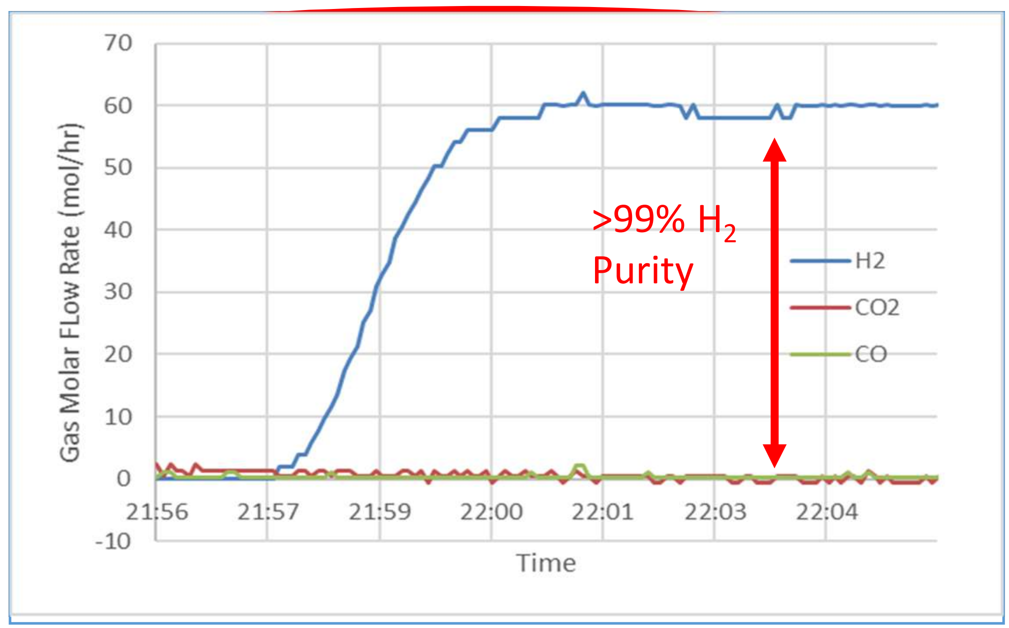

Evolution of The Ohio State Syngas Chemical Looping

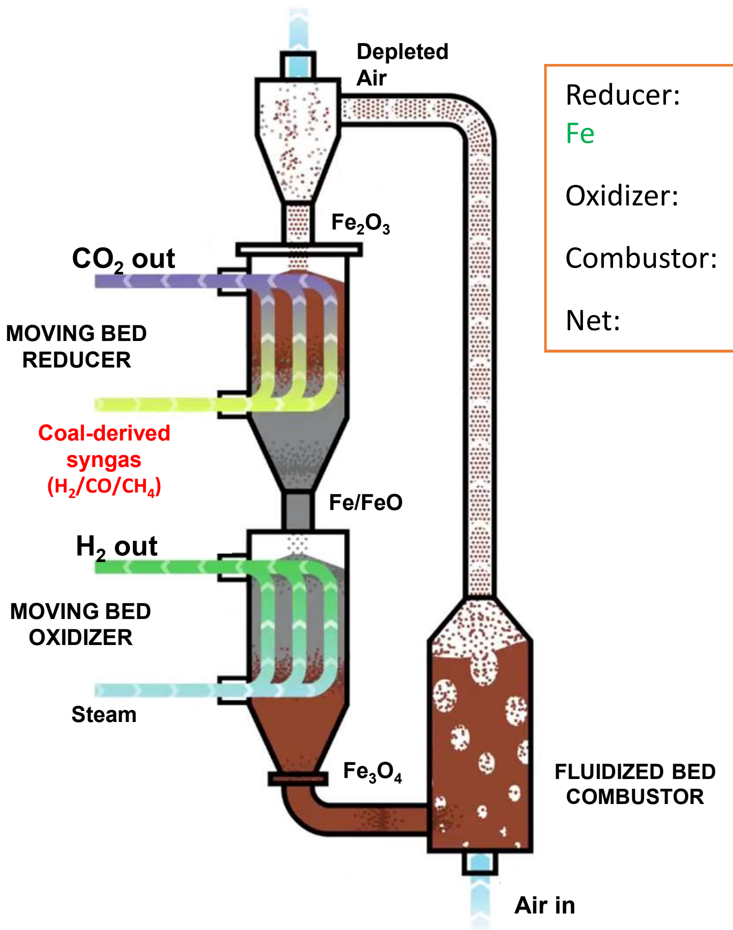

Reducer:	$C_xH_yO_z + Q + Fe_2O_3 \rightarrow CO_2 + H_2O + Fe$
Oxidizer:	$Fe + H_2O \rightarrow Fe_3O_4 + H_2 + Q$
Combustor:	$Fe_3O_4 + O_2 \rightarrow Fe_2O_3 + Q$
Net:	$C_xH_yO_z + H_2O + O_2 \rightarrow CO_2 + H_2O + H_2$

National Carbon Capture Center, Wilsonville, Alabama

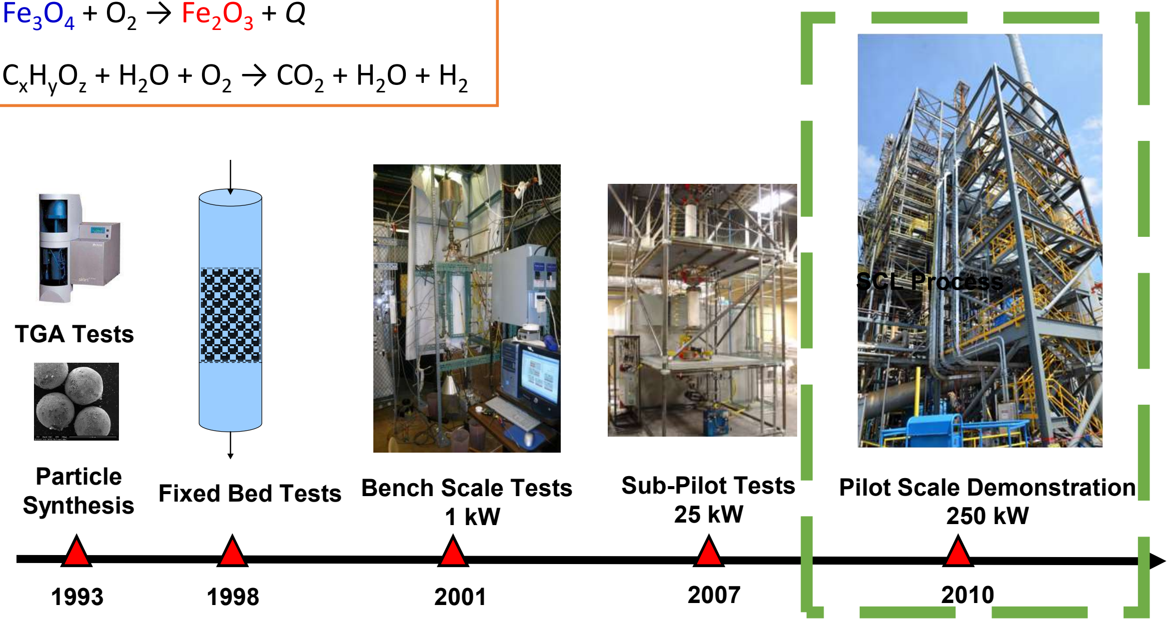

Summary of DE-FE0026334

Autonomous Process Control Concept

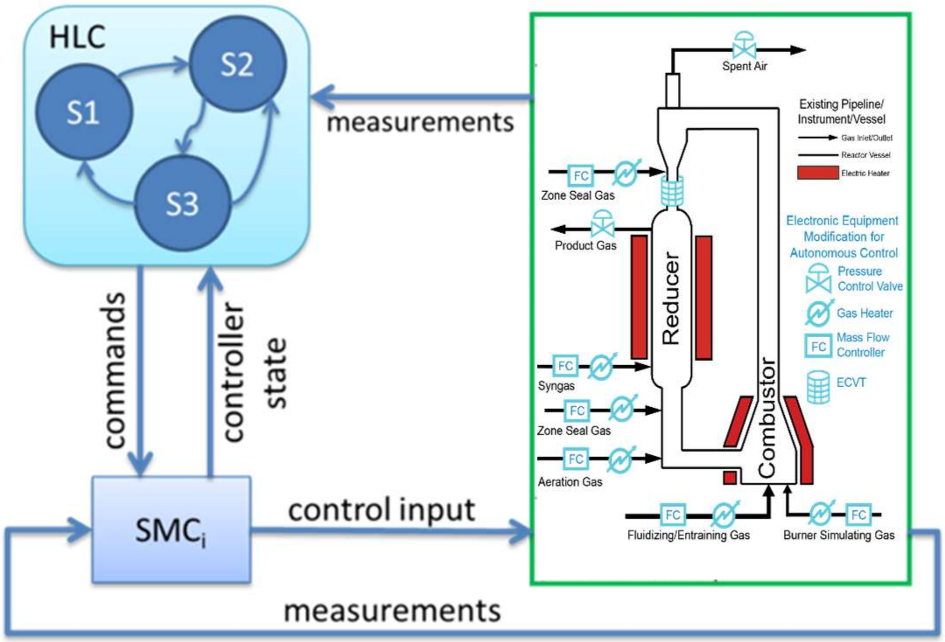

Sub-Pilot Unit

Pilot Unit

- Objective: develop an advanced process automation control architecture and imaging and optimization sensor information for the OSU chemical looping process
  - Develop HLC-SMC control scheme for process automation (**OSU ECE**)
  - Establish sensor algorithm for high temperature ECVT (**Tech4Imaging**)
  - Integrate process performance parameters with FocalPoint Optimization System (**B&W**)
  - Prepare and test process control and optimization concepts in 25 kW$_{th}$ sub-pilot test unit (**OSU CBE**)

Sliding Mode Controller (SMC)

- Advantage: State trajectory control, robustness
- Controller changes behavior as the state trajectory crosses the surface
- Exemplary mathematical form:

$$\ddot{x} + a_2 \dot{x} + a_1 x = u,$$

$$u = -M sign(s), \quad s = cx + \dot{x}, \; a_1, a_2, M, c \text{ - const}$$

- Two stages:
  - Reaching mode: to get to the sliding surface
  - Sliding mode: reduced order motion on the surface
- Disadvantage: chattering ➔
  - actuator wear-and-tear
  - potential plant excitement

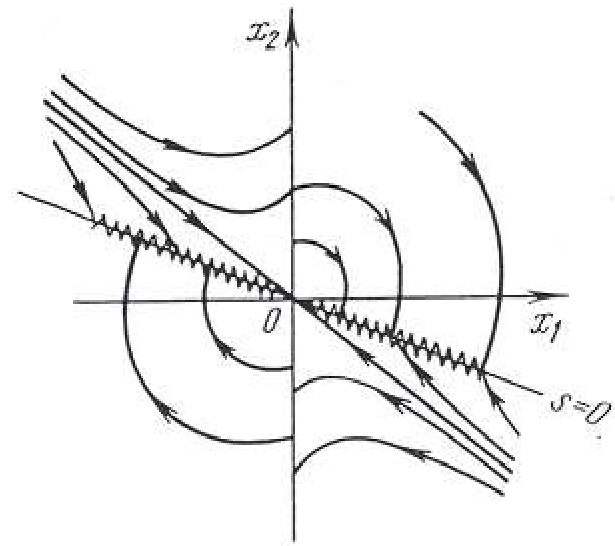

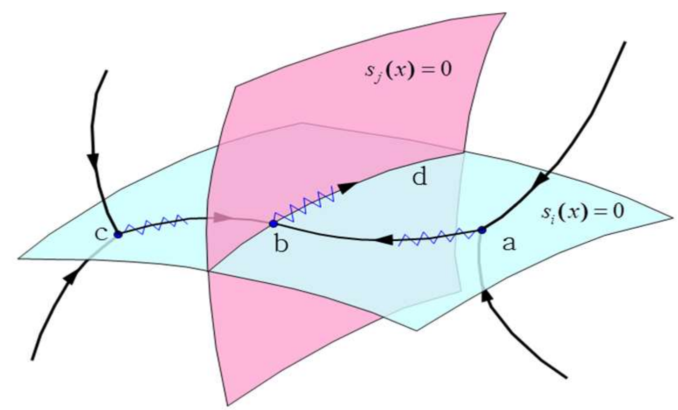

Utkin, V., "Variable structure systems with sliding modes," *Automatic Control, IEEE Transactions on* , vol.22, no.2, pp.212,222, Apr 1977

Design of adaptive M

Modified sigmoid function:

$$M = \left(b + \frac{a}{1 + e^{c - d|s|}}\right) k$$

Goal:

- Reduce chattering
- Enhance disturbance rejection

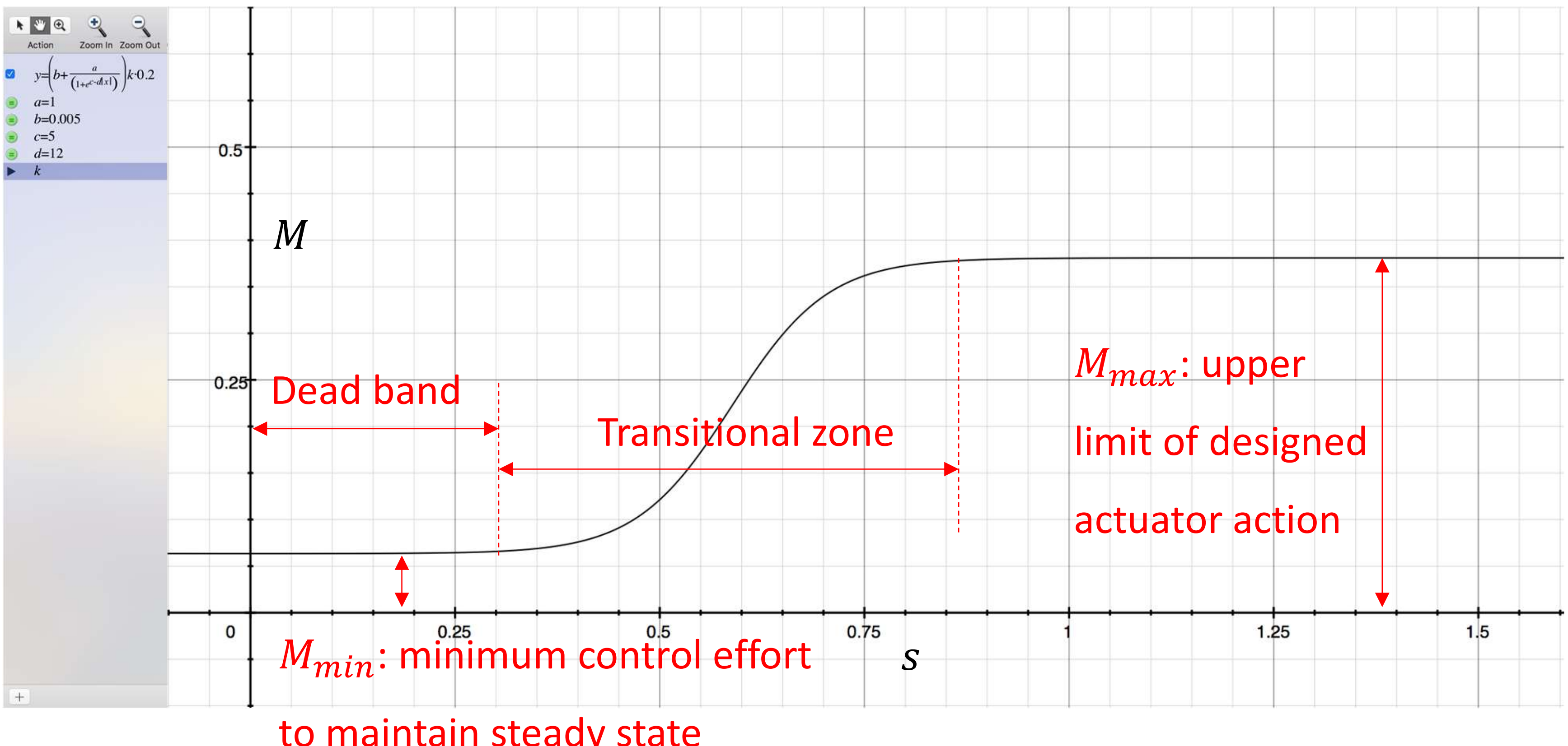

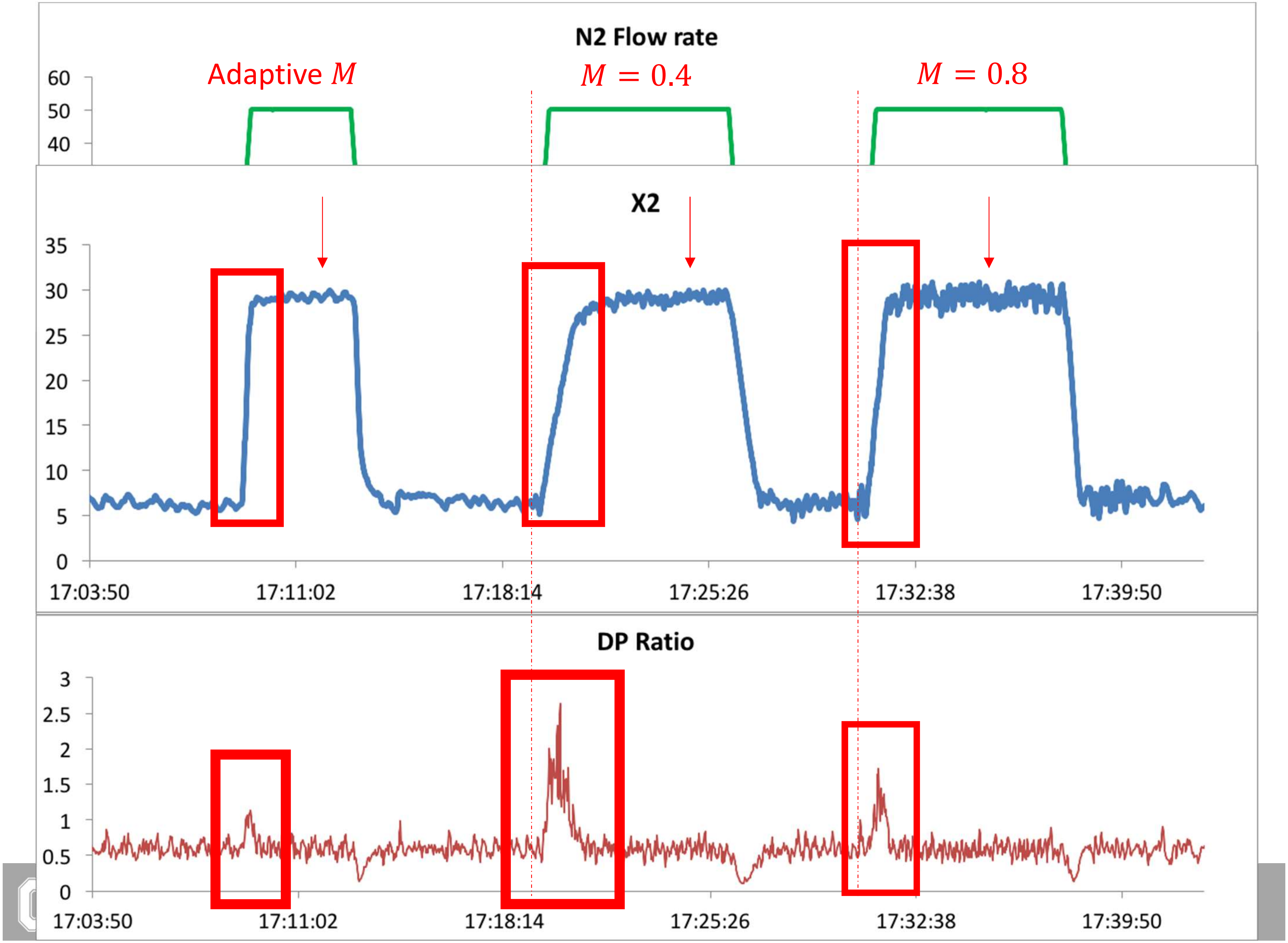
N2 Flow rate
Adaptive M
$M = 0.4$
$M = 0.8$
60
50
40
X2
35
30
25
20
15
10
5
0
17:03:50
17:11:02
17:18:14
17:25:26
17:32:38
17:39:50
DP Ratio
3
2.5
2
1.5
1
0.5
0
17:03:50
17:11:02
17:18:14
17:25:26
17:32:38
17:39:50

Implementation of automatic start-up algorithm

- Pre-set operation goals
- HLC-SMC structure
- 1-click startup for fluidization, entrainment and maintaining circulation during heat-up
- Fuel injection upon reaching reaction temperatures and operation 1-click acknowledgement

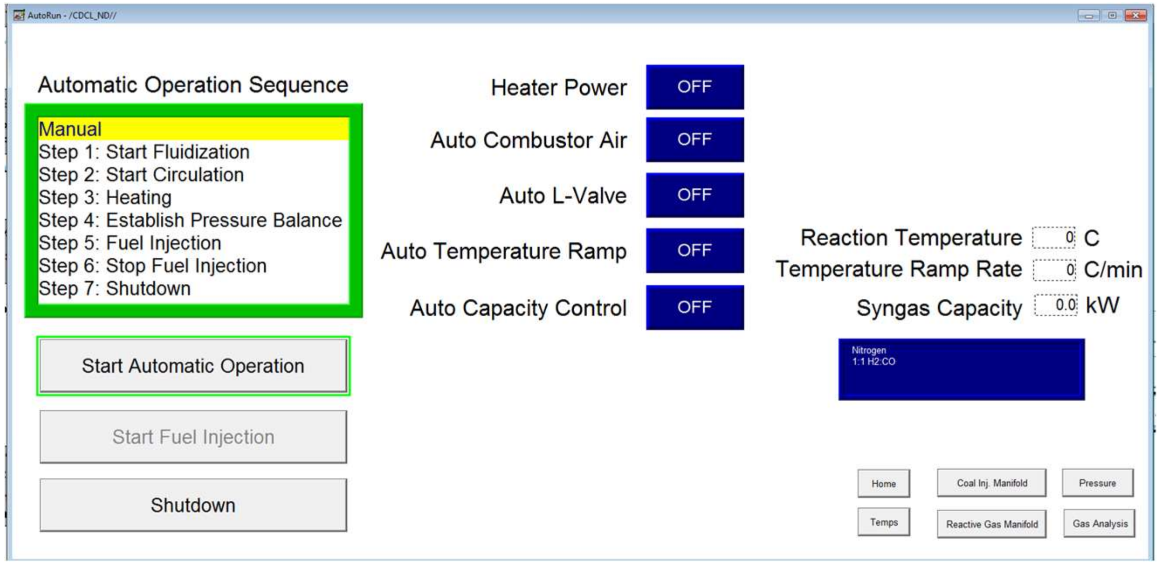

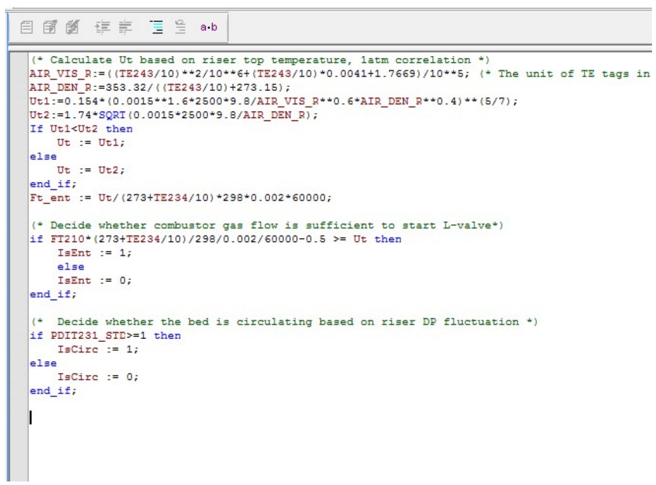

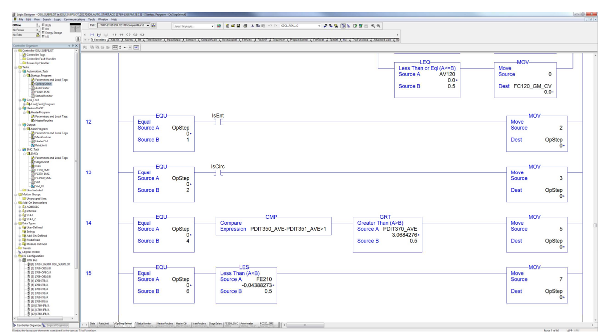

Start-up sequence test drive

- Achieved automatic startup with zero operator intervention
- Maintained oxygen carrier circulation at minimal solid flow rate using self-regulating aeration and entrainment gases

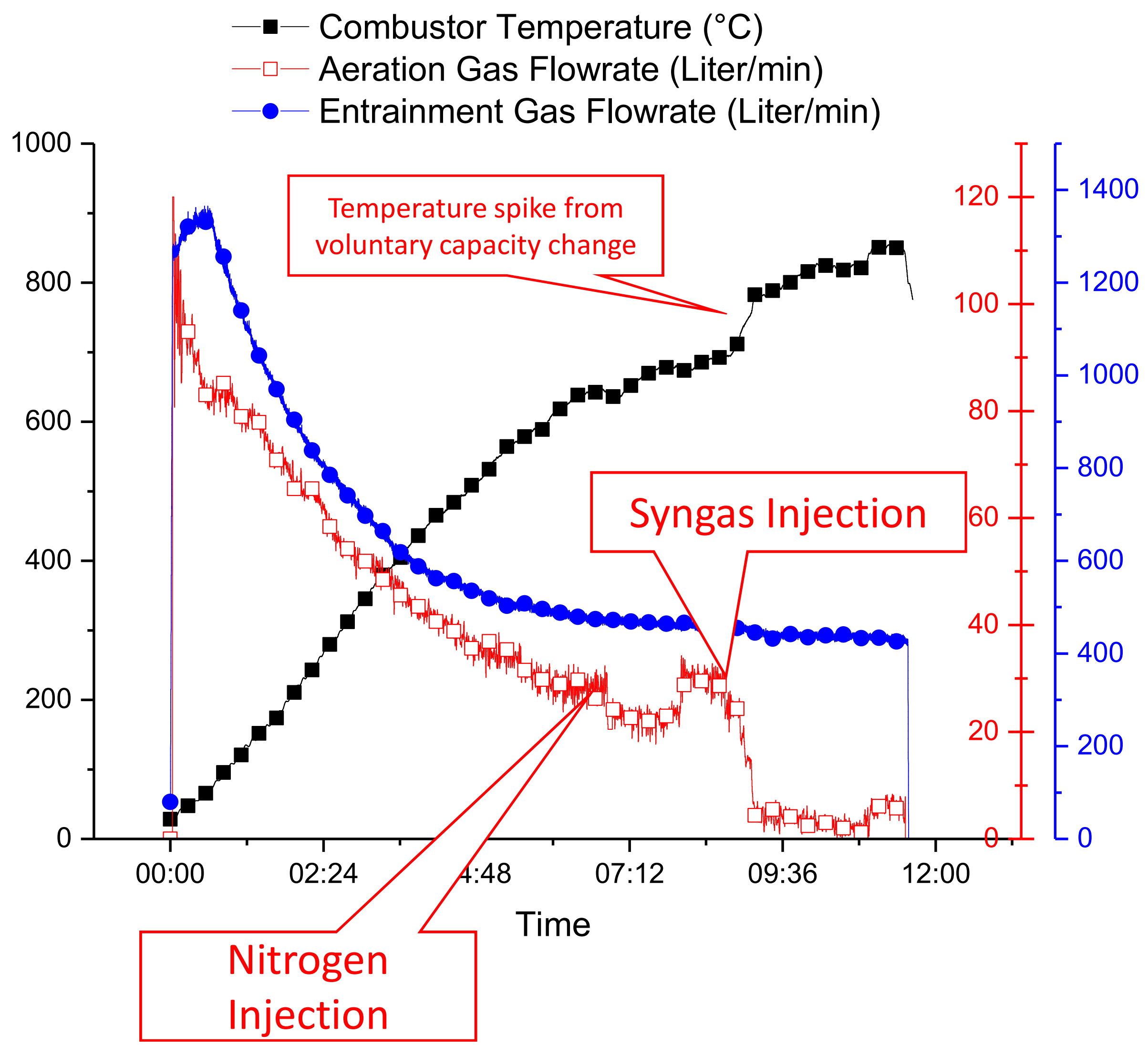

Circulation rate control

- SMCs attempt to minimize attrition by controlling circulation rate

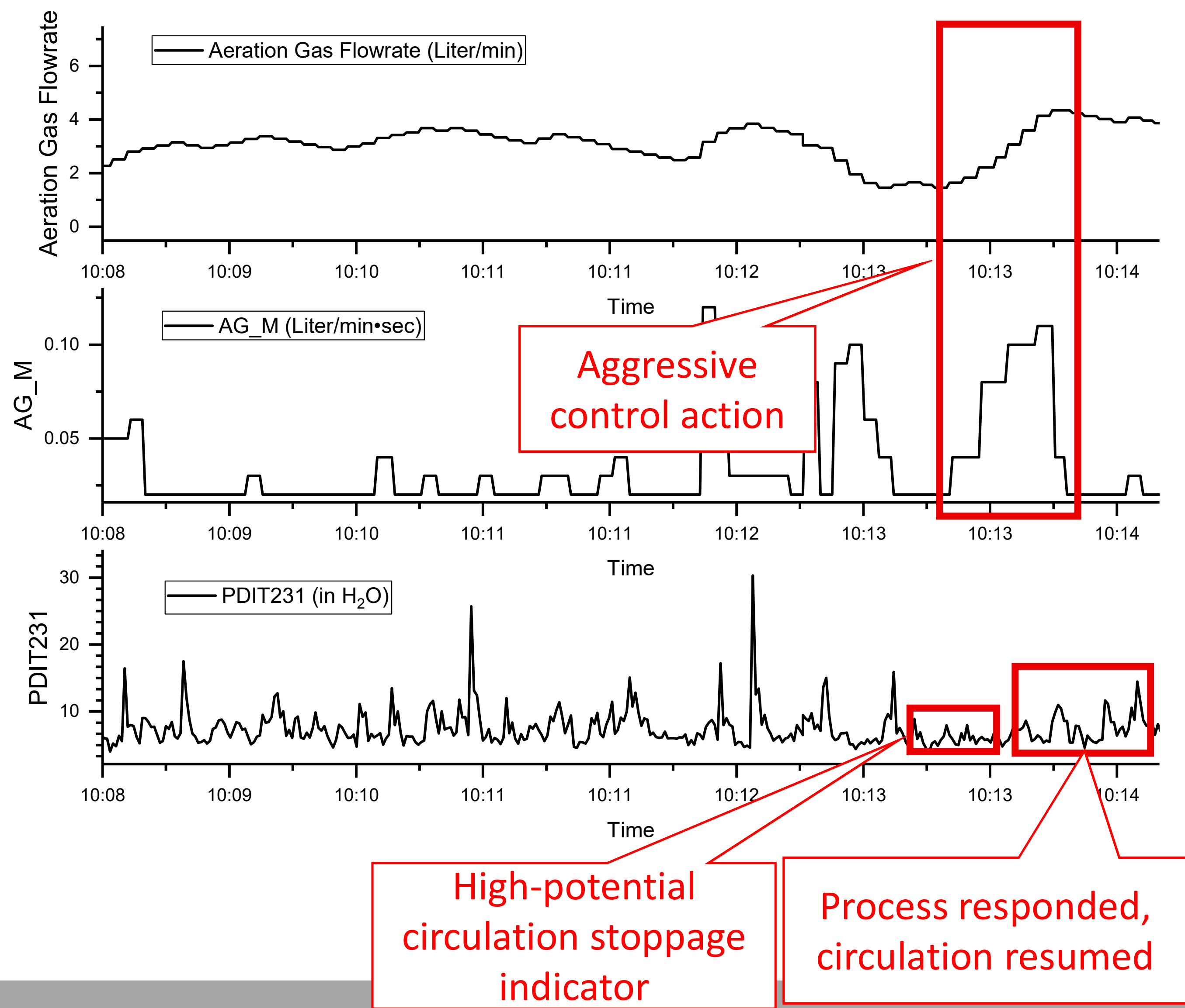

Fuel injection mode

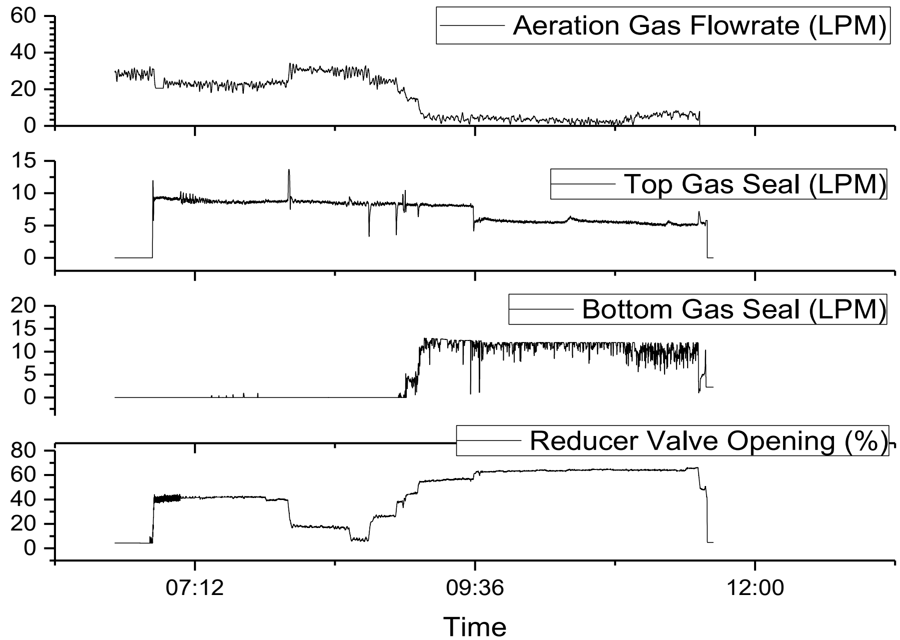

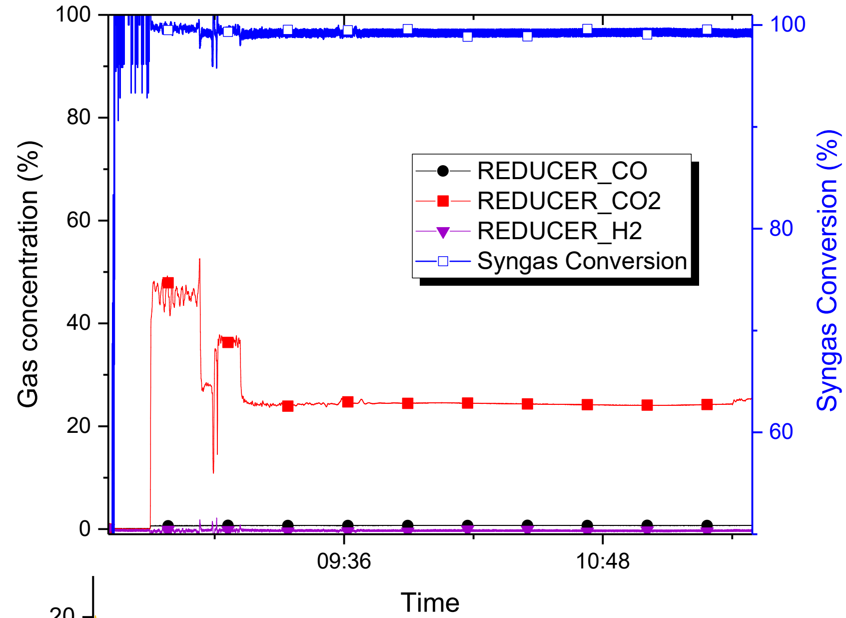

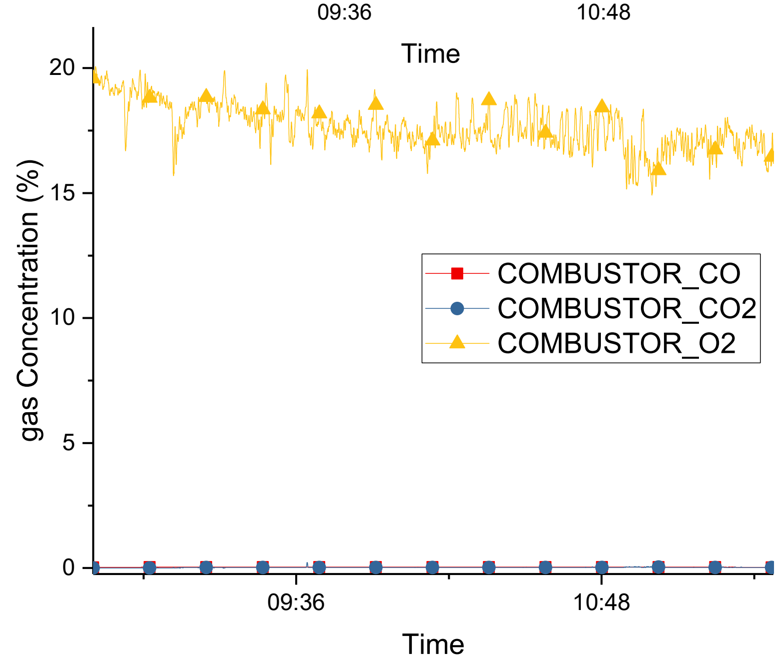

- Simultaneous control actions correctly executed by all SMCs with no operator intervention
- Achieved ~99% syngas conversion
- No gas breakthrough was observed in either reactor

SCL Pilot Unit Pressurization/Depressurization

Ramp surface:

$$u = M_2 \cdot sign(S_2)$$

$$S_2 = \frac{dP}{dt} - RR$$

$$RR: Ramp\ rate$$

SS surface:

$$u = M_3 \cdot sign(S_3)$$

$$S_2 = \frac{dP}{dt} + \left(P - P_{sp}\right) \cdot K$$

$$P_{sp} = setpoint, K = const$$

$$u = \frac{dx}{dt}$$

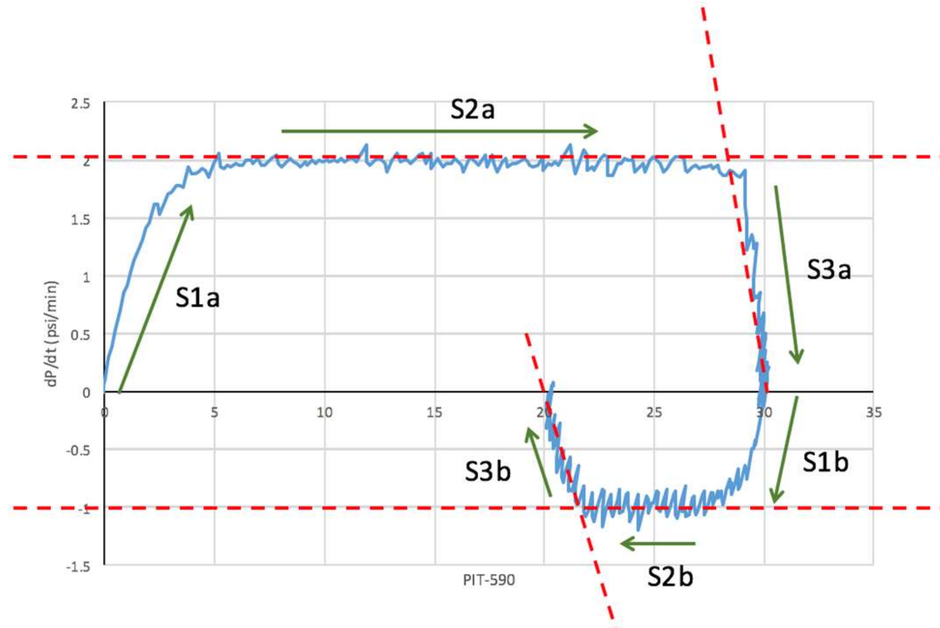

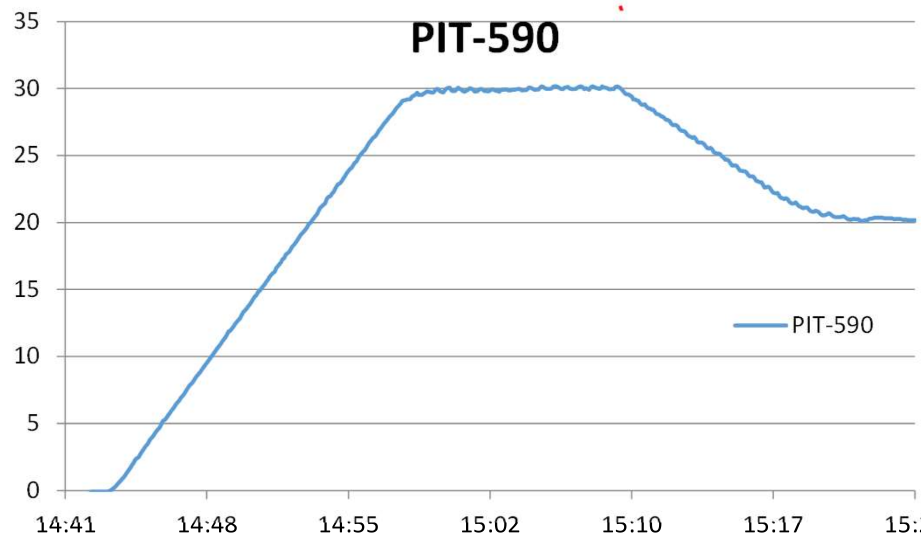

Electrical Capacitance Volume Tomography (ECVT)

Sensor Assembly

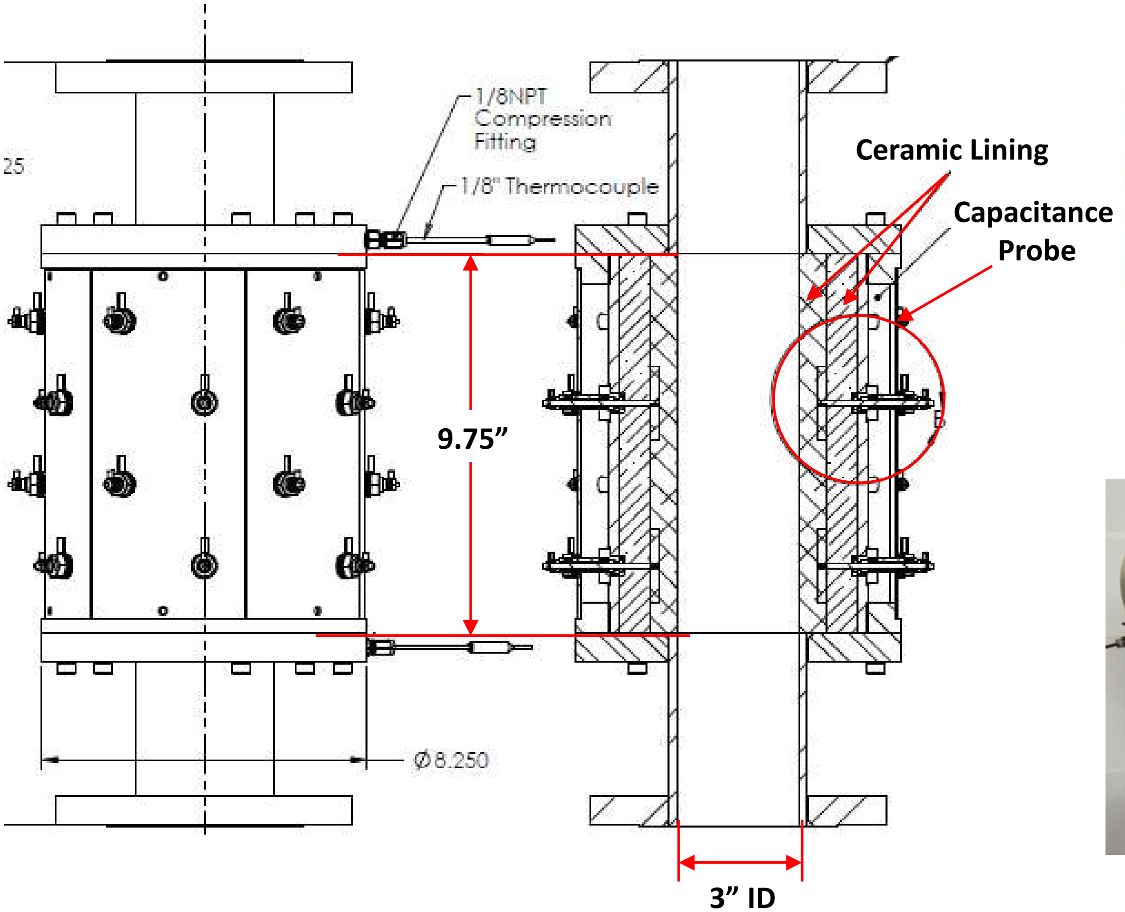

Capacitance Probe Arrangement

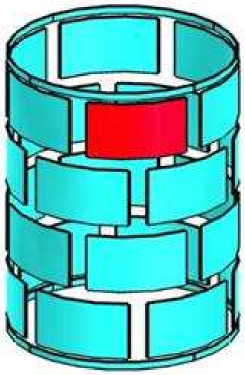

24 channel Sensor

ECVT on OSU Chemical Looping System

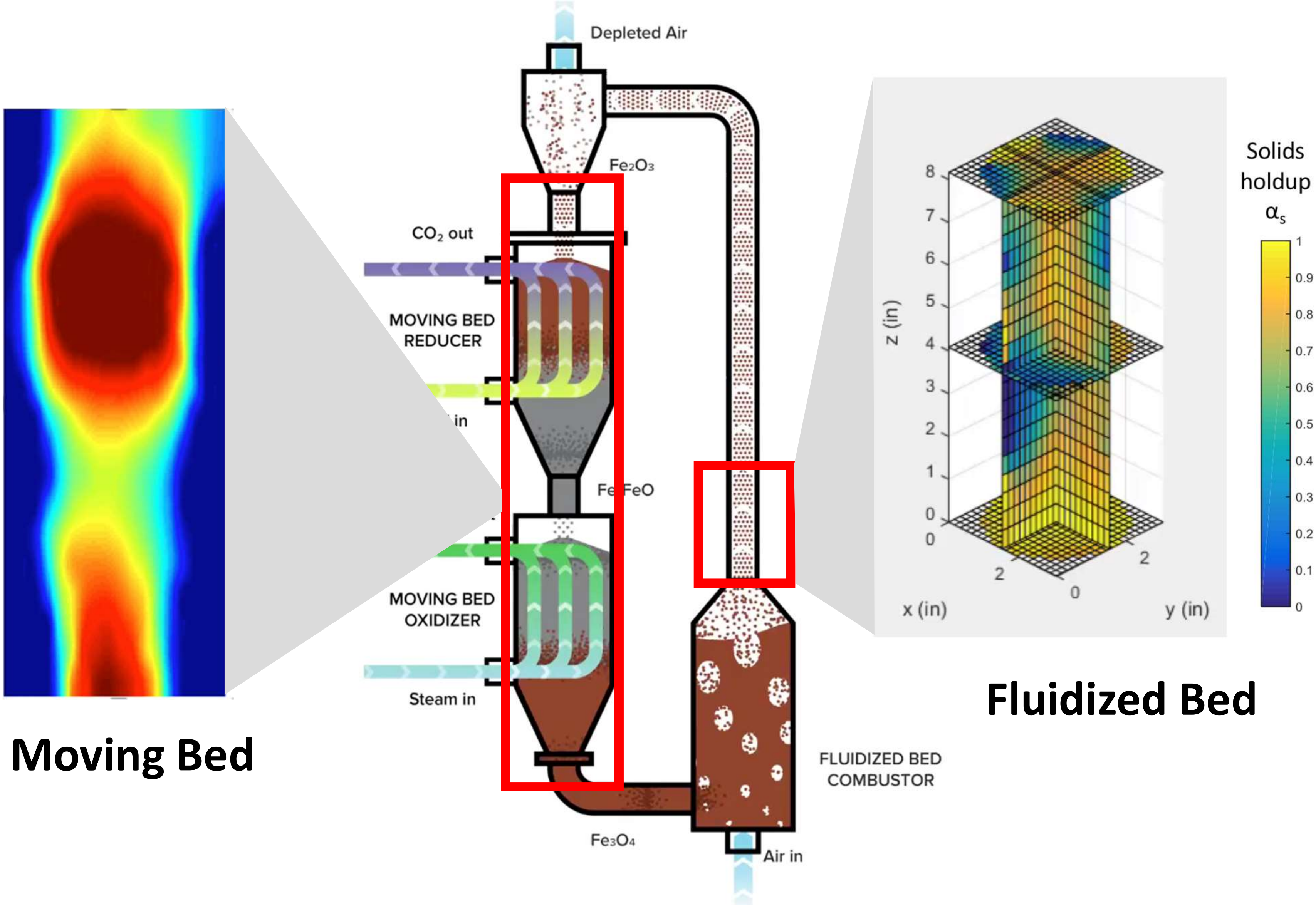

Moving Bed

Fluidized Bed

Fluidized Bed Combustor - Slug Flow 800˚C

Vertical Cross-Sectional Image

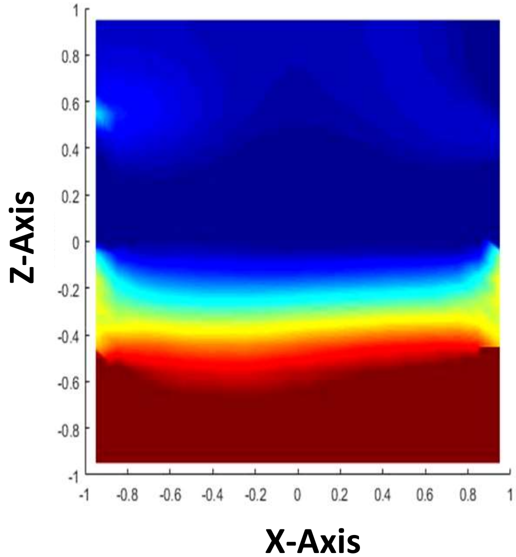

3-Dimensional Image

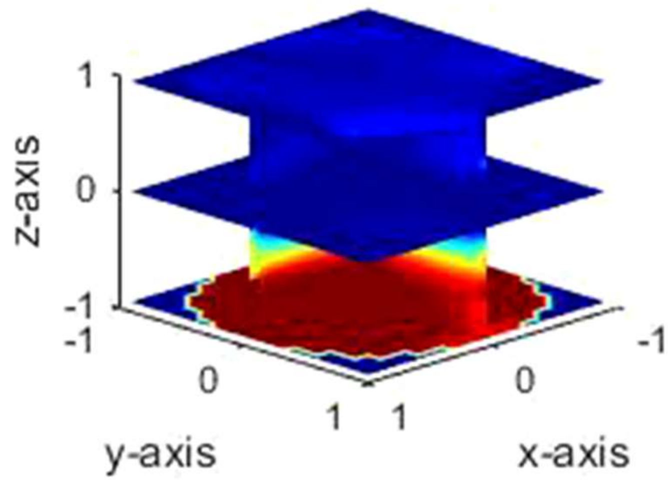

Operating Conditions

T = 800°C
Q_{Air} = 283 slpm
U_{mf} = 0.84 m/s
U = 4.07 m/s
U/U_{mf} = 4.82
d_p = 1.5mm
ρ_p = 2500 kg/m^3

Normal Plane Image

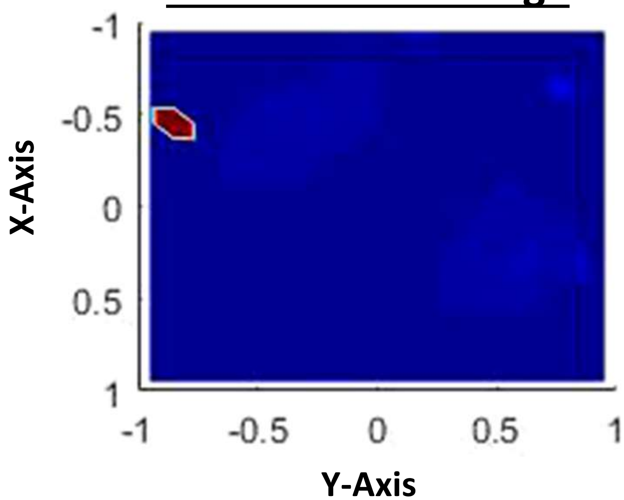

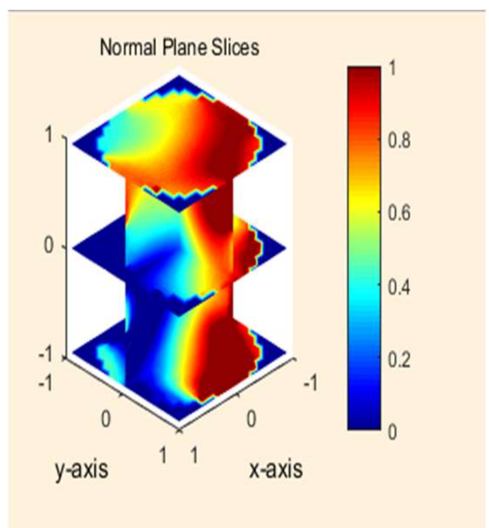

Raw Capacitance Measurement

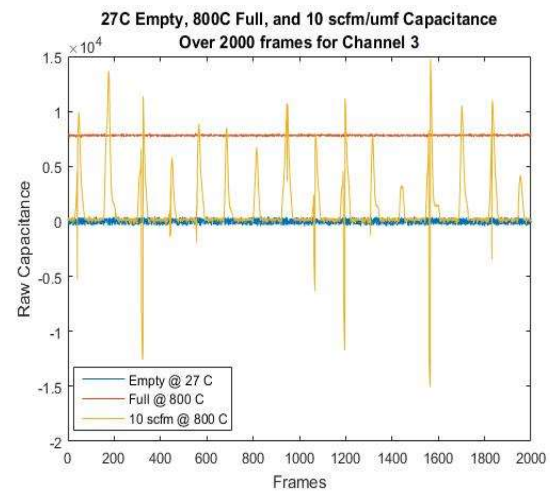

Temperature Variation of Slugging Fluidized Bed

Image Reconstruction:

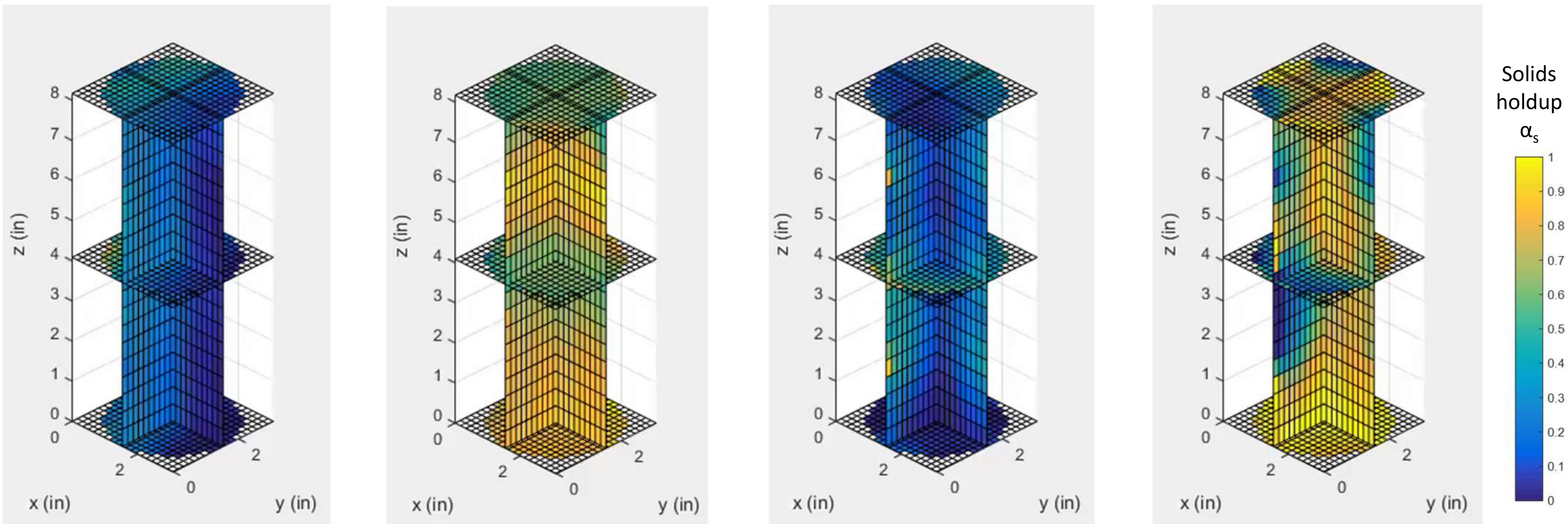

23 C, 600 slpm	335 C, 300 slpm	640 C, 220 slpm	720 C, 176 slpm
U_g-U_{mf} = 1.49	U_g-U_{mf} = 1.5	U_g-U_{mf} = 1.80	U_g-U_{mf} = 1.47

Image reconstruction frame rate: 80 Hz ~ 260 Hz

Fluidized Bed Characterization

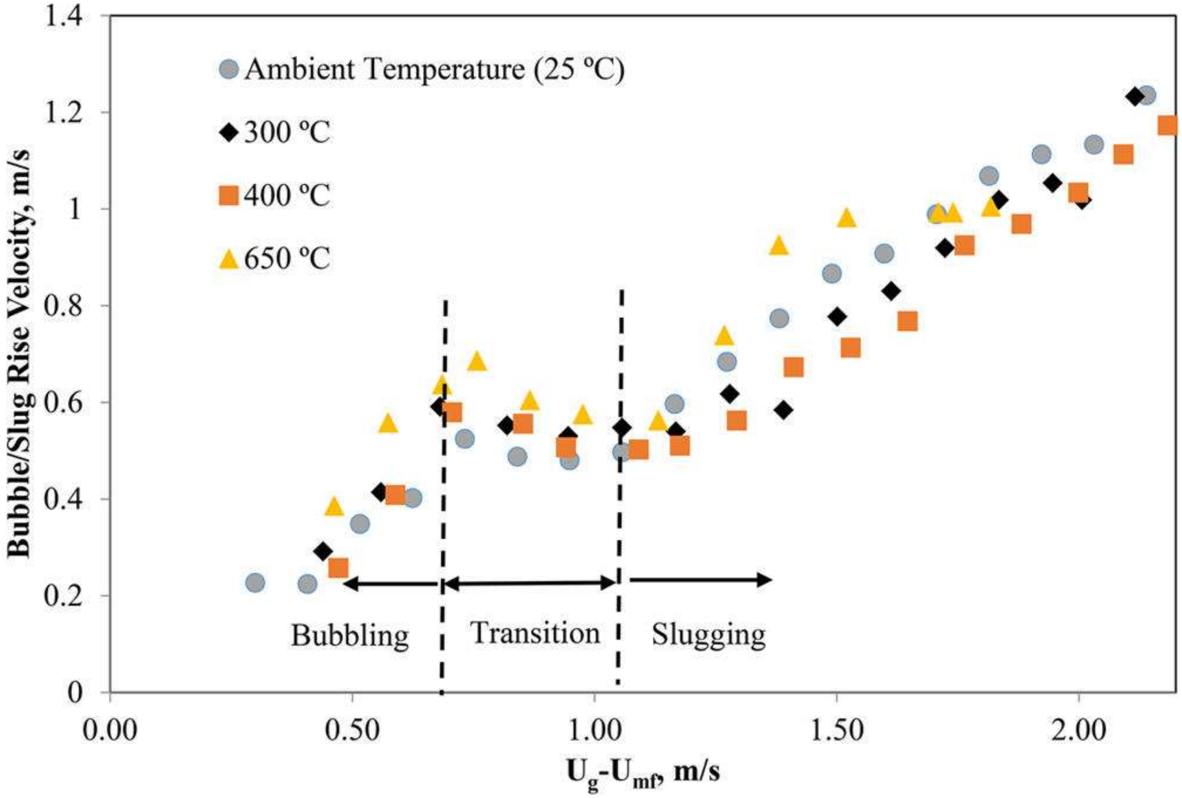

- Separate fluidization regimes identified
  - Bubbling, Slugging, and Transition Regimes
  - Bubbling – irregular gas bubbles
  - Transition – bubble coalescence and partial gas slugs
  - Slugging – fully developed gas slugs

Moving Bed Velocity - ECVT

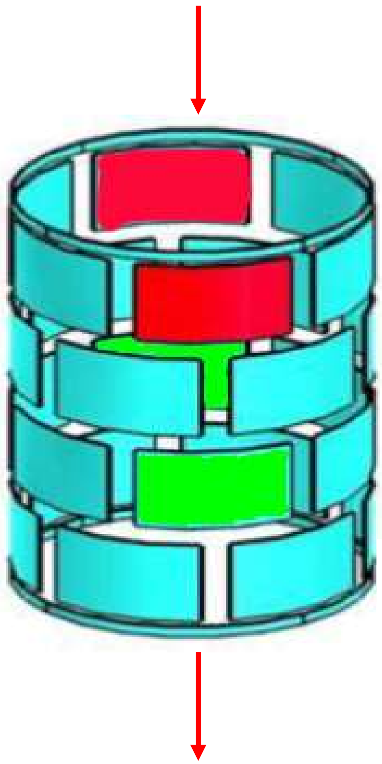

- Parallel pairs of plates at different vertical locations chosen
- Irregularities in solid holdup detected as bed moves through sensor
- Capacitance signals cross-correlated to find frame 'lag'
- Using sensor dimensions and data framerate, linear velocity can be extracted

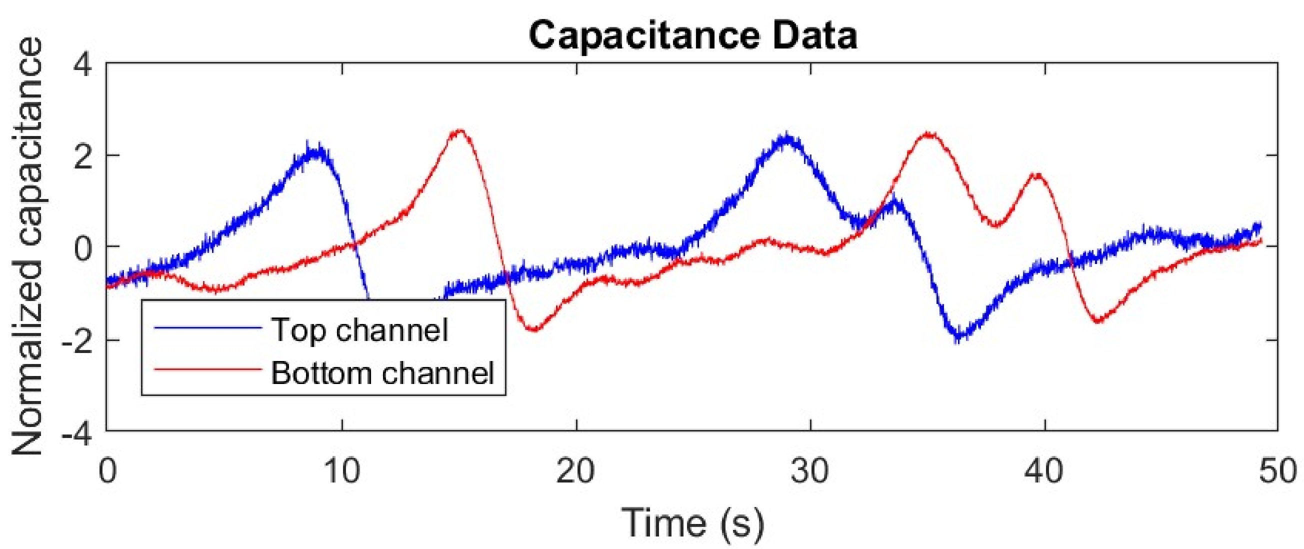

Moving Bed Velocity – Cross Correlation

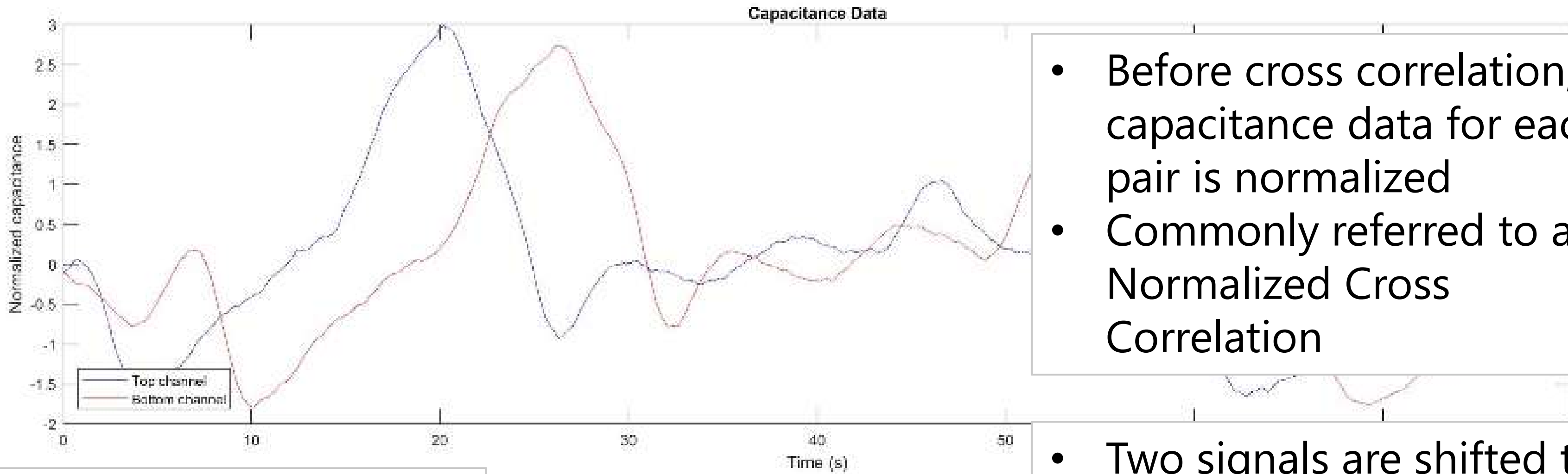

- Before cross correlation, capacitance data for each pair is normalized
- Commonly referred to as Normalized Cross Correlation

$$\hat{C}_1 = \frac{C_1 - \bar{C}_1}{\sqrt{\frac{1}{N-1}\sum_i |C_{1i} - \bar{C}_1|}}$$

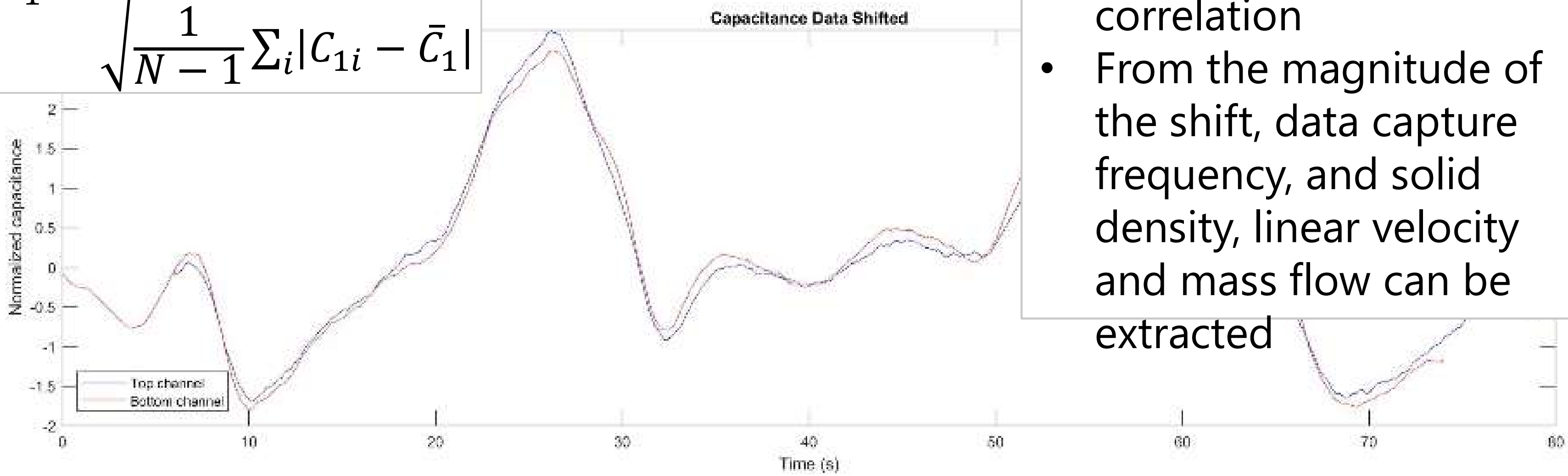

- Two signals are shifted to find the maximum cross correlation
- From the magnitude of the shift, data capture frequency, and solid density, linear velocity and mass flow can be extracted

Moving Bed Velocity – Image Reconstruction

Raw Image

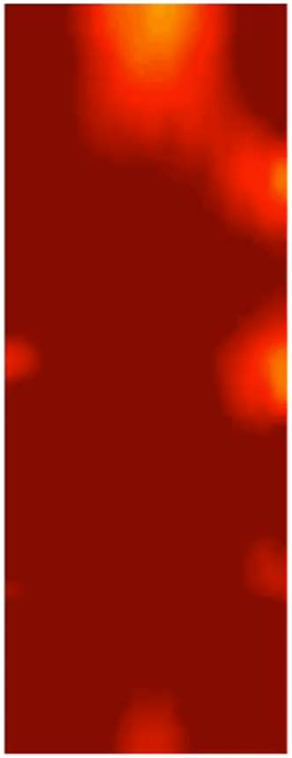

Enhanced Color Contrast

Processed

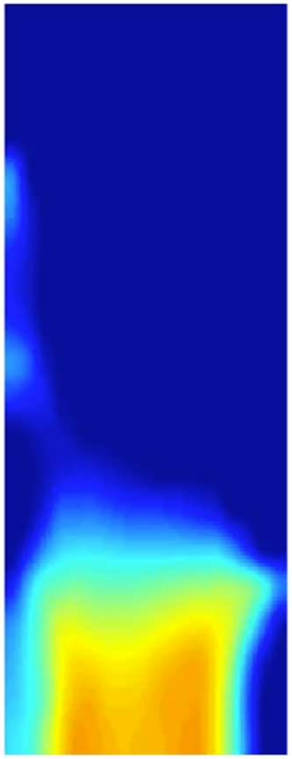

Moving Bed Velocity – Frequency Effect & Results

- High frequency generally generates noisier signals, which leads to non-matching capacitances patterns in half of the trials (*)
- Low frequency signals generally show clear patterns, which consistently allow accurate calculation of solid linear velocities by cross correlation

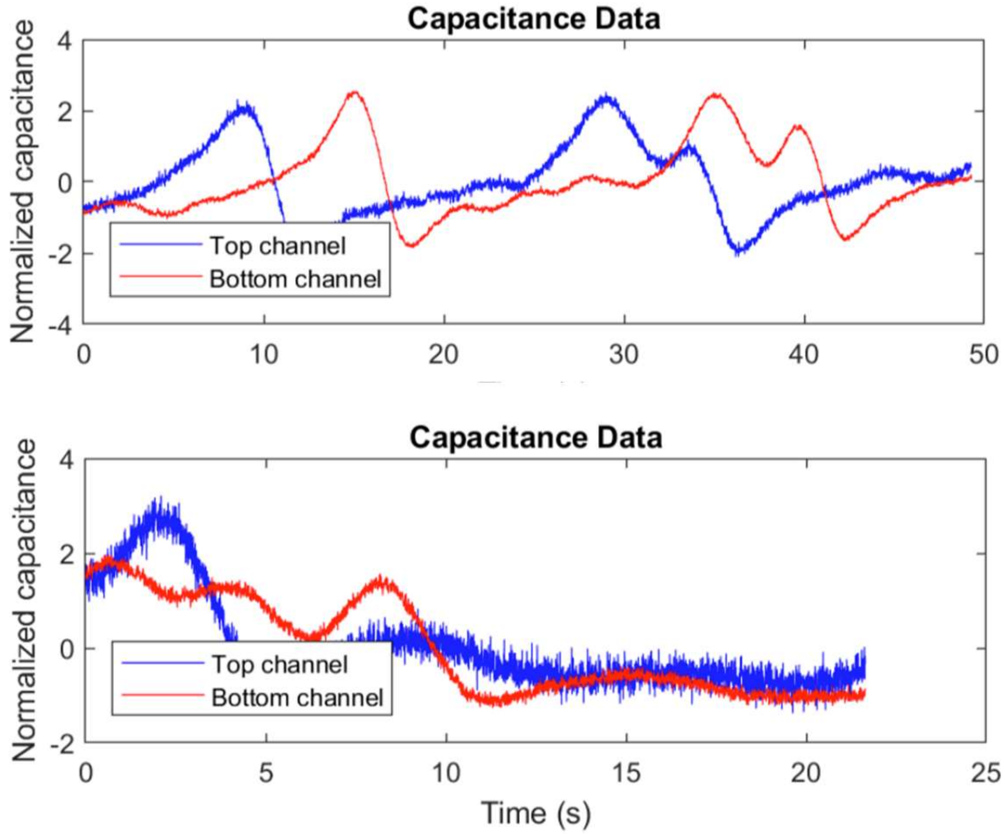

Framerate	Measured (Scale + Timer)	Calculated (ECVT)
81.16 Hz	1.62 cm/s	1.66 cm/s
184.81 Hz	1.62 cm/s	1.62 cm/s*

Moving Bed Velocity - Plate Pairing Effect

Framerate	Measured
81.16 Hz	1.62 cm/s

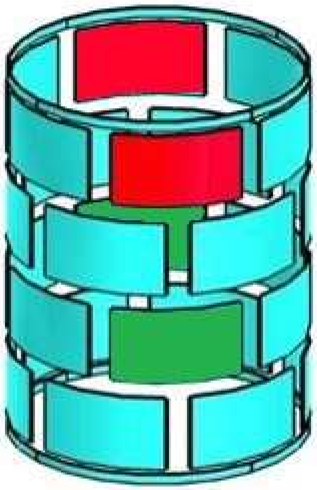

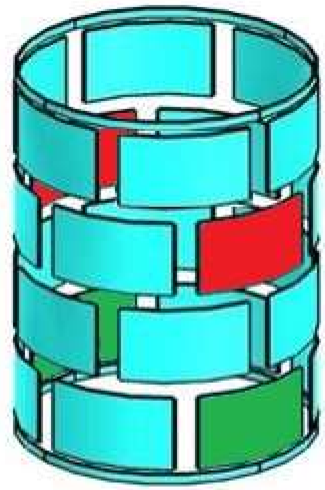

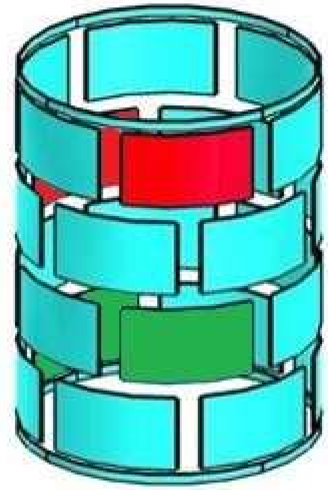

Plates	Velocity (cm/s)
1,4 – 13,16	1.66
2,5 – 14,17	1.65
3,6 – 15,18	1.65

Plates	Velocity (cm/s)
7,10 – 19,22	1.72
8,11 – 20,23	1.73
9,12 – 21,24	1.72

Plates	Velocity (cm/s)
1,9 – 13,21	1.72
2,10 – 14,22	1.89
3,11 – 15,23	1.75

Project Achievements

- Autonomous startup, steady-state operation and shutdown
  - Implemented hybrid HLC-SMC structure
  - Designed system successfully carried out complete operation sequence with minimal human intervention
- ECVT Solid flow control development
  - Developed two different applications of ECVT to non–intrusively monitor different gas-solid flow patterns at high temperatures

Remaining Task

- Optimization Software
  - Designed optimization problem : minimizing aeration/entrainment gas while maximizing gas conversion
  - Preliminary data obtained. Analyzing data and revising program

Acknowledgements

- DOE/NETL
- Ohio Development Service Agency: Gregory Payne

Research Group Members

This presentation was prepared as an account of work sponsored by an agency of the United States Government. Neither the United States Government nor any agency thereof, nor any of their employees, makes any warranty, express or implied, or assumes any legal liability or responsibilities for the accuracy, completeness, or usefulness of any information, apparatus, product, or process disclosed, or represents that its use would not infringe privately owned rights. Reference herein to any specific commercial product, process, or service by trade name, trademark, manufacturer, or otherwise does not necessarily constitute or imply its endorsement, recommendation, or favoring by the United States Government or any agency thereof. The views and opinions of the authors expressed herein do not necessarily state or reflect those of United States Government or any thereof.

Dynamic Modeling

- Ergun Equation

$$DP_{360} = \frac{150\mu_{N_2}L_{361}}{d_p^2}\frac{(1-\epsilon)^2}{\epsilon^3}u_{361} + \frac{1.75\rho_{360}L_{361}}{d_p}\frac{(1-\epsilon)}{\epsilon^3}u_{361}|u_{361}|$$

- Valve Equation

$$\begin{cases} F_{490} = 3.455\times10^{-5}\left(mol\cdot s^{-1}\cdot Tg_{490}^{\frac{1}{2}}\cdot Pa^{-1}\right)\times C_v\cdot x_{490}\cdot\sqrt{\frac{P_{490}^2-P_0^2}{Tg_{491}S_g}} \quad when\ \frac{P_{490}}{P_0} < 1.89 \\ F_{490} = 2.934\times10^{-5}\left(mol\cdot s^{-1}\cdot Tg_{490}^{\frac{1}{2}}\cdot Pa^{-1}\right)\times C_v\cdot x_{490}\cdot P_{490}\sqrt{\frac{1}{Tg_{491}S_g}} \quad when\ \frac{P_{490}}{P_0} > 1.89 \end{cases}$$

- Gas Mass Balance

$$\frac{dP_O}{dt} = \frac{R\cdot Tg_{490}\cdot(F_{420}+F_{371}+F_{362}-F_{490})}{V} + \frac{P_O}{Tg_{490}}\cdot\frac{dTg_{490}}{dt}$$

- Combustor/Riser Correlation

$$DP_C = \begin{cases} H_C\times\rho_s\times\alpha_C\times g & if \quad u_{gC} > u_{mf} \\ L\times(150\frac{(1-\varepsilon)^2}{\varepsilon^3}\frac{\mu_{air}u_{gC}}{d_p^2}+1.75\frac{1-\varepsilon}{\varepsilon^3}\frac{\rho_{gC}u_{gC}^2}{d_p^2}) & if \quad u_{gC}\le u_{mf} \end{cases}$$

$$\alpha_c = 0.63\,(1+\frac{21.4(u_g-u_{mf})^{0.738}d_s^{1.006}\rho_s^{0.376}}{u_{mf}^{0.937}(M_g\frac{P_{11}}{P_a})^{0.126}})^{-1}$$

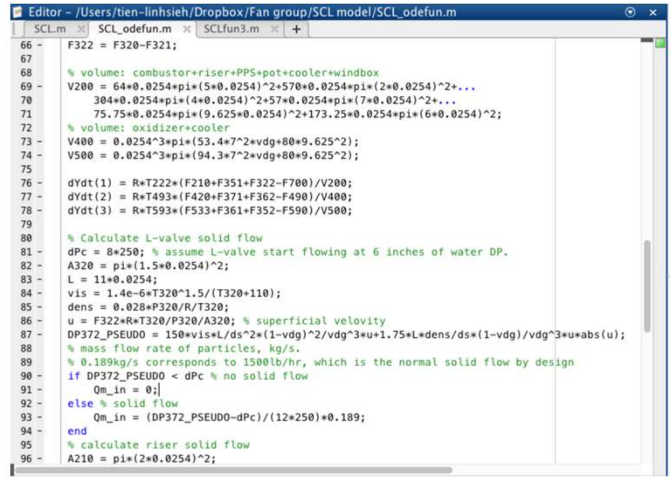

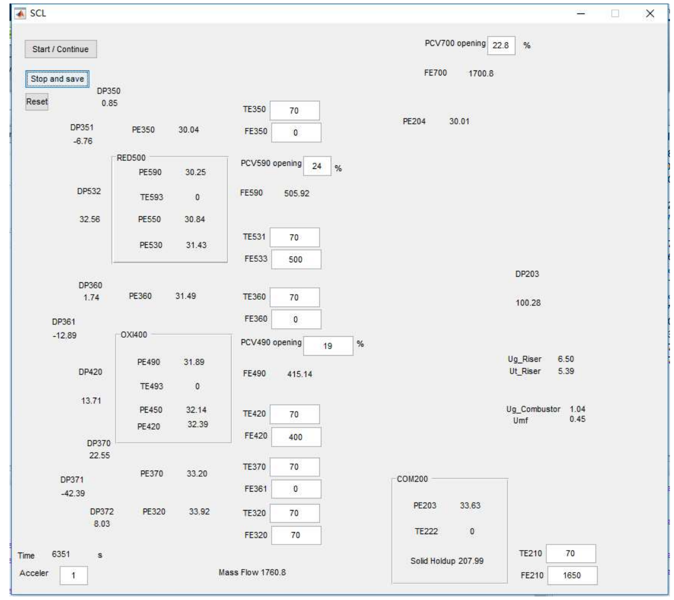

Phase Plane

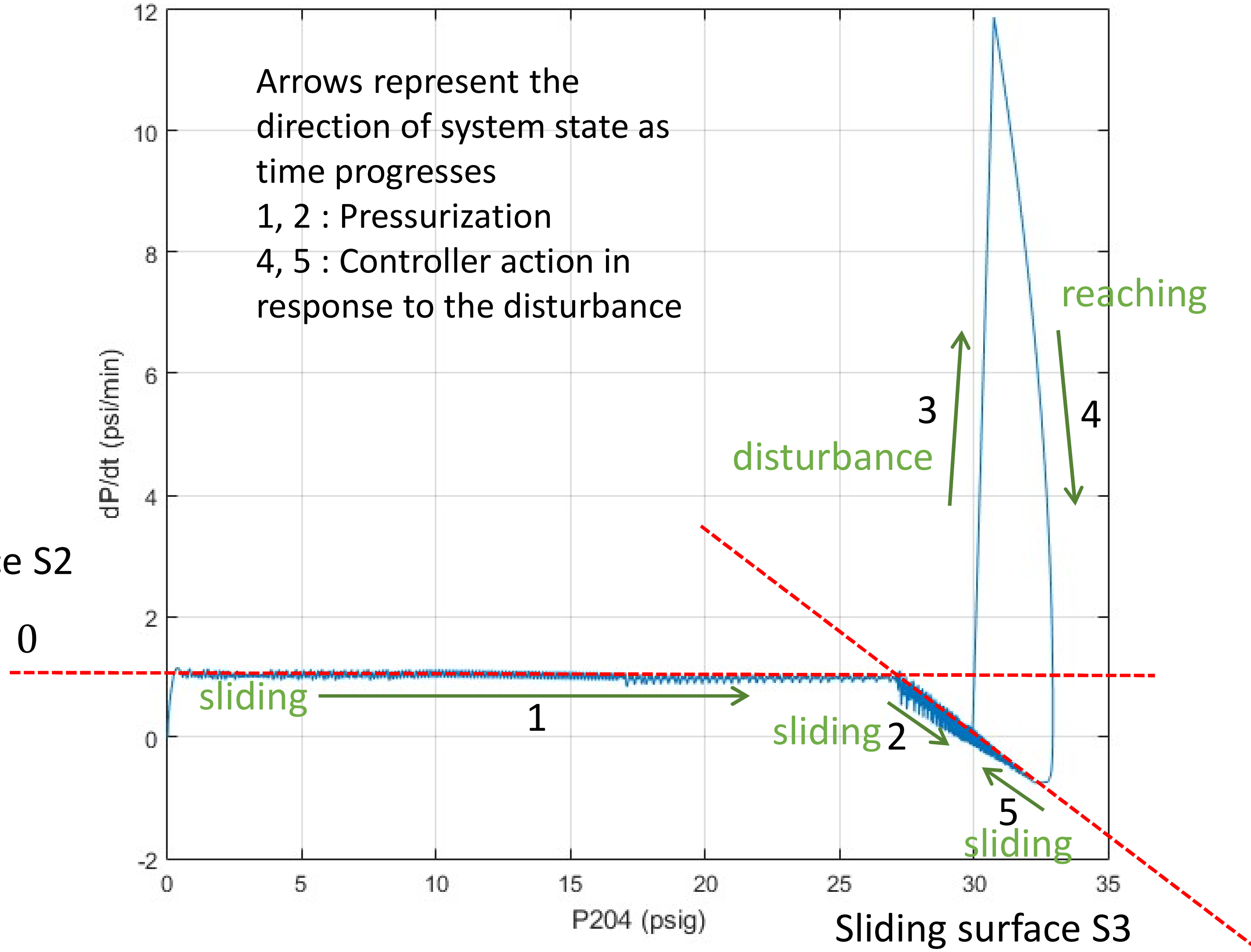

Sliding surface S2

$$\frac{dP}{dt} - 1 = 0$$

Sliding surface S3

$$\frac{dP}{dt} + \frac{P-30}{3} = 0$$

Matlab simulation of a sliding mode controller design for pressure control

- Control law: rate of valve opening change
  - $u = \frac{dx}{dt}$
- S2 Controller:
  - $u = M_2 \cdot sign(S_2)$
  - $S_2 = \frac{dP}{dt} - RR$
  - $RR = 1\, psi/min$
- S3 Controller:
  - $u = M_3 \cdot sign(S_3)$
  - $S_3 = \frac{dP}{dt} + (P - P_{sp}) \cdot K$
  - $P_{sp} = 30psig, K = \frac{1}{3} min^{-1}$

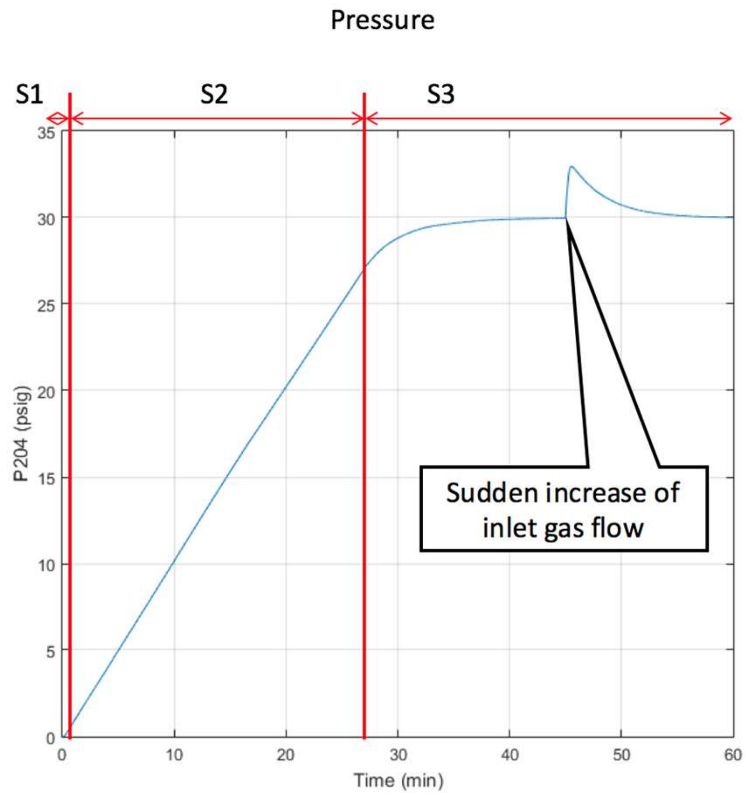

Design of adaptive M

Modified sigmoid function:

$$M = \left(b + \frac{a}{1 + e^{c-d|s|}}\right)k$$

Goal:

- Reduce ch
- Enhance c

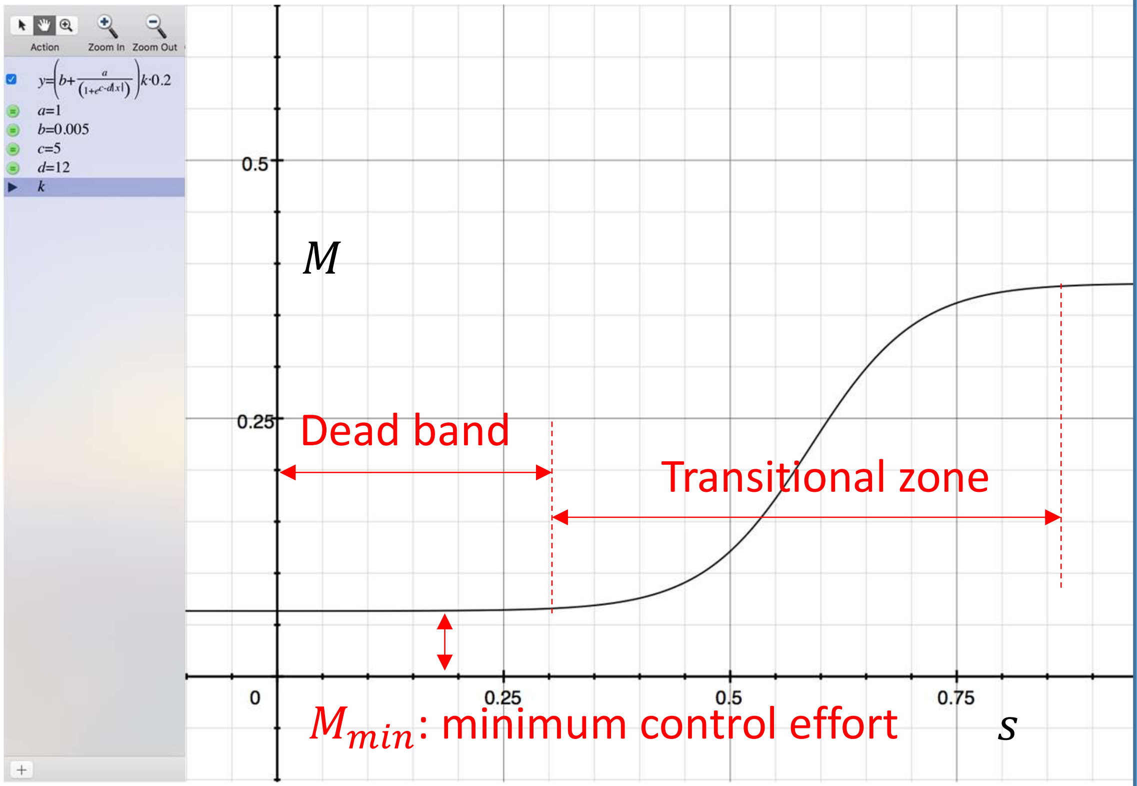

M_{min}: minimum control effort

to maintain steady state

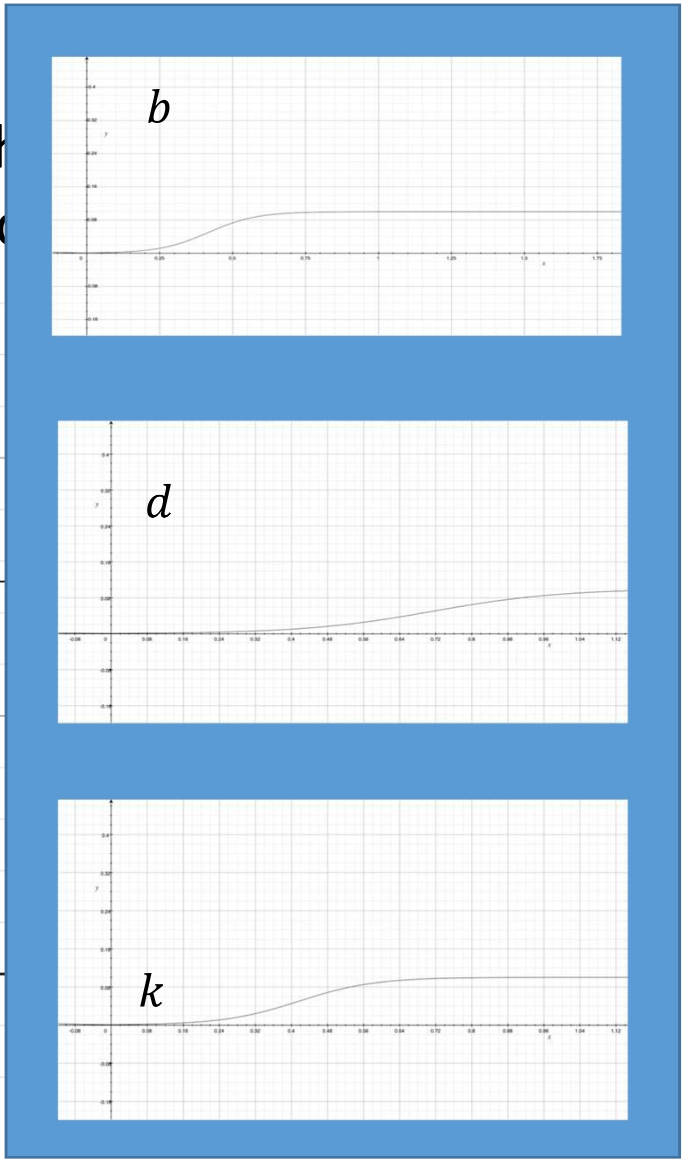

Sliding Mode Controller for Pilot Unit System Pressure Control

- Vessel model:
  - Consider the reactor as a single tank with one inlet and one outlet
  - Isothermal
  - $\frac{dP}{dt} = \frac{RT}{V} \times \left(F_{210} - x \cdot f(P_{204})\right)$
  - x is valve opening ZYT-700, $x \cdot f(P_{204})$ is the valve flow equation:
  - $f(P) = \begin{cases} C_v \cdot Y \cdot N \cdot P \cdot \sqrt{\frac{P-P_0}{PM_wT}} & if\ \frac{P-P_0}{P} < 0.64 \\ C_v \cdot Y \cdot N \cdot P \cdot \sqrt{\frac{0.64}{M_wT}} & if\ \frac{P-P_0}{P} \geq 0.64 \end{cases}$
  - Initial condition: P_{204} = 0 psig, T = 300K, ZYT-700 = 0
  - F_{210} increase from 0 to 1000 lb/hr at 1 lb/hr/s
  - F_{210} sudden increase from 1000 to 1300 at t=45min
  - Pressurization in three stages:
    - S1: outlet closed, start gas flow, till dP/dt > 1 psi/min
    - S2: pressurize at dP/dt = 1 psi/min, until
    - S3: gradually slow down pressurization, and maintain pressure at 30 psig

Fuel injection mode

- Nitrogen injection to verify behaviors for individual SMCs
- Extreme capacity change to test disturbance rejection performance

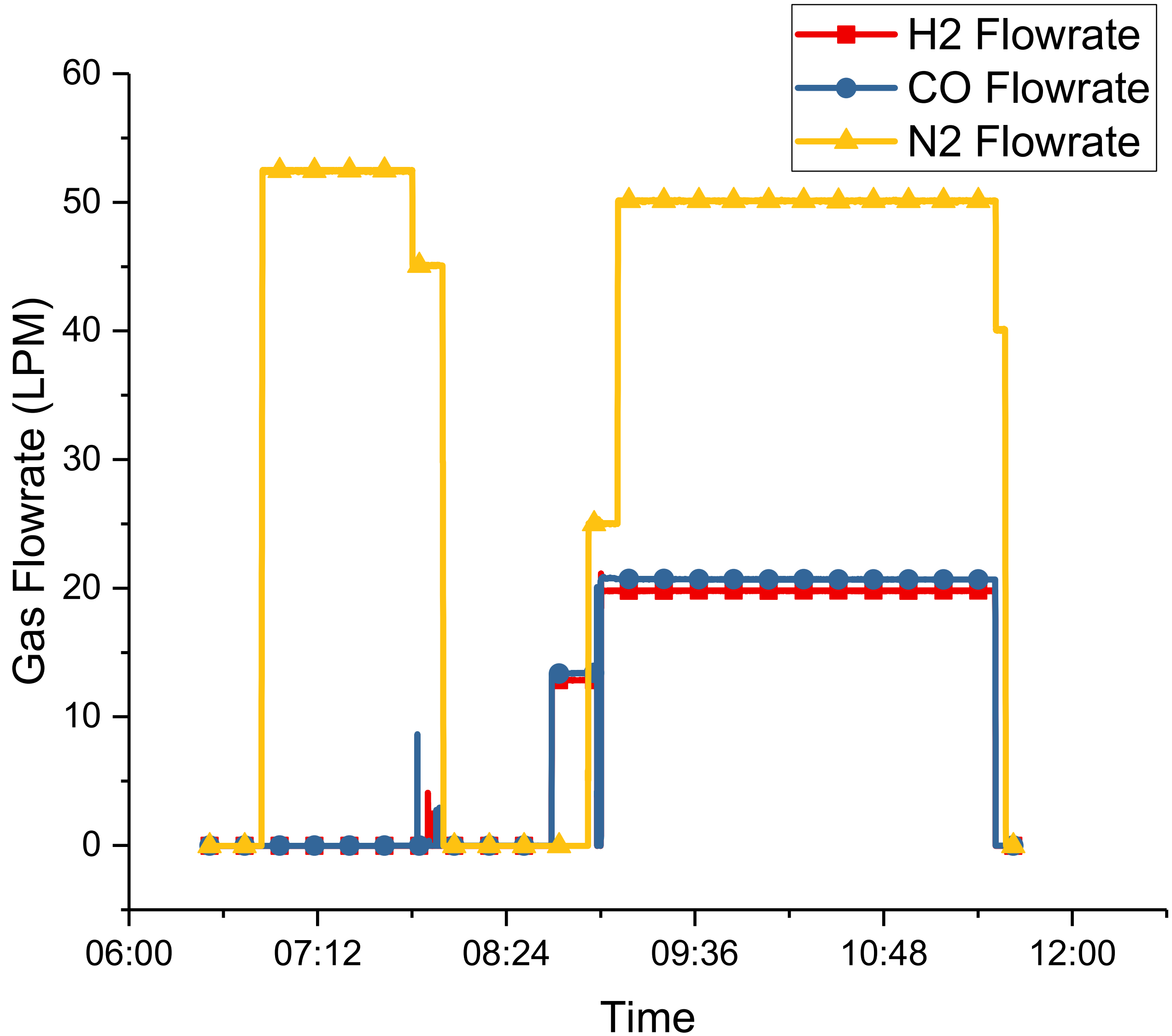

SMC Response to Capacity Change